Appl. Phys. A (2016) 122:39
DOI 10.1007/s00339-015-9534-0

Applied Physics A
Materials Science & Processing

INVITED PAPER

Nonlinear-optical frequency-doubling metareflector: pulsed regime

A. K. Popov[1] · **S. A. Myslivets**[2,3]

Received: 13 August 2015 / Accepted: 15 December 2015 / Published online: 6 January 2016

Abstract The properties of backward-wave second-harmonic metareflector operating in pulse regime are investigated. It is made of metamaterial which enables phase matching of contra-propagating fundamental and second-harmonic waves. References are given to the works that prove such a possibility. Physical principles underlying differences in the proposed and standard settings as well as between continuous-wave and pulsed regimes are discussed. Pulsed regime is more practicable and has a broader scope of applications. A set of partial differential equations which describe such a reflector with the account for losses are solved numerically. It is shown that unlike second-harmonic generation in standard settings, contra-propagating pulse of second harmonic may become much longer than the incident fundamental one and the difference grows with decrease in the input pulse length as compared to thickness of the metaslab. The revealed properties are important for applications and may manifest themselves beyond the optical wavelength range.

✉ A. K. Popov
popov@purdue.edu;
https://nanohub.org/groups/nlo/popov

[1] Birck Nanotechnology Center, Purdue University, West Lafayette, IN 47907, USA

[2] Institute of Physics, Siberian Branch of the Russian Academy of Sciences, Krasnoyarsk, Russian Federation 660036

[3] Siberian Federal University, Krasnoyarsk, Russian Federation 660041

1 Introduction

Light can be described as a set of traveling electromagnetic waves (EMWs) with phase velocity $\mathbf{v}_{\text{ph}}$ of each wave directed along the wave vector $\mathbf{k}$ whereas its energy flux is represented by the Poynting vector $\mathbf{S}$:

$$\mathbf{v}_{\text{ph}} = (\mathbf{k}/k)(c/n), \quad \mathbf{S} = (c/4\pi)[\mathbf{E} \times \mathbf{H}] = (c^2\mathbf{k}/4\pi\omega\epsilon)\mathbf{H}^2 = (c^2\mathbf{k}/4\pi\omega\mu)E^2. \tag{1}$$

Here, c is speed of light, n is refractive index of the propagation medium, $\mathbf{E}$ and $\mathbf{H}$ are electric and magnetic components of the wave. Refractive index is determined by electric permittivity ϵ and magnetic permeability μ of the medium at corresponding frequency. In all naturally occurring materials, $\epsilon > 0$, $\mu > 0$, $n = \sqrt{\mu\epsilon}$ and vectors $\mathbf{S}$ and $\mathbf{k}$ are codirected. In the case of $\epsilon < 0$ and $\mu < 0$, refractive index becomes negative, $n = -\sqrt{\mu\epsilon}$, and vectors $\mathbf{S}$ and $\mathbf{k}$—*contra-directed*. Such waves are referred to as *backward* EMW (BEMW). Backward light became achievable only recently owing to the advent of nanotechnology and optical metamaterials that has led to revolutionary breakthrough in the concept and in numerous applications of linear optics [1]. Extraordinary coherent (i.e., phase dependent) nonlinear-optical (NLO) processes were predicted in [2–5] for the cases of coupled ordinary and BEMW waves. Among them are second-harmonic generation (SHG) [2–4], parametric amplification and frequency-shifted nonlinear reflectivity [4–6]. Metamaterials (MM) are artificially designed and engineered materials, which can have properties unattainable in nature. Current mainstream in fabricating negative-index MM (NIM) relies on engineering of LC nanocircuits—plasmonic mesoatoms at the nanoscale with negative electromagnetic response. Extraordinary NLO frequency-converting propagation

processes predicted in NIMs have been experimentally realized to date in the microwave transmission lines [7] and in the plasmonic optical MM [8]. However, a different, more general approach to engineering the MM, which can provide *coexistence and phase matching* of ordinary and BEMW, and its particular realization were proposed in [9–11]. The proposed paradigm exploits specially designed *hyperbolic* MM, which support both *positive and negative* spatial dispersions. Such an approach *does not* require the engineering of optical magnetism in order to ensure the appearance of BEMW. The underlying idea is as follows. In a loss-free isotropic medium, energy flux **S** and group velocity $\mathbf{v}_g$ are related as

$$\mathbf{S} = \mathbf{v}_g U,\ \mathbf{v}_g = \mathrm{grad}_{\mathbf{k}}\omega(\mathbf{k}). \tag{2}$$

Here, U is energy density attributed to EMW. It is seen that the group velocity and the energy flux become directed *against* the wave vector **k** if the dispersion $\partial\omega/\partial k$ is negative. Generally, negative spatial dispersion $\partial\omega/\partial k < 0$ may appear even in fully dielectric materials with particular composition of its structural elements [12, 13]. This paradigm opens an entirely novel research and application avenue. Various particular realizations of negative dispersion were proposed in [9–11, 14, 15]. Basically, many hyperbolic MM and specially designed waveguides can support BW electromagnetic modes, see, e.g., [16–19]. This opens new avenues for creation of BW photonic devices with unparalleled functional properties. As regards coherent nonlinear-optical propagation processes, critically important is to provide for coexistence of coupled ordinary and backward waves whose frequencies and wave vectors satisfy energy and momentum conservation law (phase matching). Such possibilities were described in Ref. [9–11].

This paper is to investigate unusual behavior of BW SHG in the pulse regime. We show that conversion efficiency and properties of generated SH pulses depend on the ratio of the input fundamental harmonic (FH) pulse length to thickness of the NLO MM slab. Losses are included in the consideration.

2 Basic equations

As noted, properties of SHG will be investigated for the cases where one of the coupled waves is ordinary and the other one is BW. To achieve phase matching, wave vectors of the fundamental and the SH waves must be codirected. This means that in BW setting pulse of the SH will propagate *against* the pulse of fundamental radiation. Corresponding basic equations are as follows. Electric and magnetic components of the waves and corresponding nonlinear polarizations at ω_1 and at $\omega_2 = 2\omega_1$ are defined as

$$\{\mathcal{E},\mathcal{H}\}_j = \mathrm{Re}\{E,H\}_j \exp\{i(k_j z - \omega_j t)\},$$
$$\{\mathcal{P},\mathcal{M}\}_j^{NL} = \mathrm{Re}\{P,M\}_j^{NL} \exp\{i(\widetilde{k}_j z - \omega_j t)\}, \tag{3}$$

$$\{P,M\}_1^{NL} = \chi_{e,m,1}^{(2)}\{E,H\}_2\{E,H\}_1^*,$$
$$\{P,M\}_2^{NL} = \chi_{e,m,2}^{(2)}\{E,H\}_1^2,\ 2\chi_{e,m,2}^{(2)} = \chi_{e,m,1}^{(2)}. \tag{4}$$

Amplitude E_1 of the first harmonic (FH) and of the SH, E_2, is given by the equations:

$$s_2\frac{\partial E_2}{\partial z} + \frac{1}{v_2}\frac{\partial E_2}{\partial t} = -i\frac{k_2\omega_2^2}{\epsilon_2 c^2}4\pi\chi_{e,2}^{(2)}E_1^2\exp(-i\Delta k z) - \frac{\alpha_2}{2}E_2, \tag{5}$$

$$s_1\frac{\partial E_1}{\partial z} + \frac{1}{v_1}\frac{\partial E_1}{\partial t} = -i\frac{k_1\omega_1^2}{\epsilon_1 c^2}8\pi\chi_{e,1}^{(2)*}E_1^*E_2\exp(i\Delta k z) - \frac{\alpha_1}{2}E_1. \tag{6}$$

Here, $v_i > 0$ and $\alpha_{1,2}$ are group velocities and absorption indices at the corresponding frequencies, $\chi_{\mathrm{eff}}^{(2)} = \chi_{e,2}^{(2)}$ is effective nonlinear susceptibility, and $\Delta k = k_2 - 2k_1$. Parameter $s_j = 1$ for ordinary, and $s_j = -1$ for backward wave. With account for $k^2 = n^2(\omega/c)^2$, $n_1 = s_1\sqrt{\epsilon_1\mu_1}$, $n_2 = s_2\sqrt{\epsilon_2\mu_2}$, we introduce amplitudes $e_j = \sqrt{|\epsilon_j|/k_j}E_j$, $a_j = e_i/e_{10}$, coupling parameters æ$= \sqrt{k_1k_2/|\epsilon_1\epsilon_2|}4\pi\chi_{\mathrm{eff}}^{(2)}$ and $g =$ æE_{10}, loss and phase mismatch parameters $\widetilde{\alpha}_{1,2} = a_{1,2}L$ and $\Delta\widetilde{k} = \Delta k l$, slub thickness $d = L/l$, position $\xi = z/l$ and time instant $\tau = t/\Delta\tau$. It is assumed that $E_{j0} = E_j(z=0)$, $l = v_1\Delta\tau$ is the pump pulse length, and $\Delta\tau$ is duration of the input fundamental pulse. Quantities $|a_j|^2$ are proportional to the time-dependent photon fluxes. Then Eqs. (5) and (6) are written as

$$s_2\frac{\partial a_2}{\partial\xi} + \frac{v_1}{v_2}\frac{\partial a_2}{\partial\tau} = -igla_1^2\exp(-i\Delta\widetilde{k}\xi) - \frac{\widetilde{\alpha}_2}{2d}a_2, \tag{7}$$

$$s_1\frac{\partial a_1}{\partial\xi} + \frac{\partial a_1}{\partial\tau} = -i2g^*la_1^*a_2\exp(i\Delta\widetilde{k}\xi) - \frac{\widetilde{\alpha}_1}{2d}a_1. \tag{8}$$

In the case of magnetic nonlinearity, $\chi_{\mathrm{eff}}^{(2)} = \chi_{m,2}^{(2)}$, equations for amplitudes H_j take the form:

$$s_2\frac{\partial H_2}{\partial z} + \frac{1}{v_2}\frac{\partial H_2}{\partial t} = -i\frac{k_2\omega_2^2}{\mu_2 c^2}4\pi\chi_{m,2}^{(2)}H_1^2\exp(-i\Delta k z) - \frac{\alpha_2}{2}H_2, \tag{9}$$

$$s_1\frac{\partial H_1}{\partial z} + \frac{1}{v_1}\frac{\partial H_1}{\partial t} = -i\frac{k_1\omega_1^2}{\mu_1 c^2}8\pi\chi_{m,1}^{(2)*}H_1^*H_2\exp(i\Delta k z) - \frac{\alpha_1}{2}H_1. \tag{10}$$

Then, equations for amplitudes $a_j = m_i/m_{10}$, where $m_j = \sqrt{|\mu_j|/k_j}H_j$, take the form of (7) and (8), with

coupling parameters given by $æ = \sqrt{k_1 k_2/|\mu_1\mu_2|}4\pi\chi^{(2)}_{\text{eff}}$ and $g = æH_{10}$. In both cases, $z_0 = g^{-1}$ is characteristic medium length required for significant NLO energy conversion. Only most favorable case of the exact phase matching $\Delta k = 0$ will be considered below.

3 Extraordinary properties of the backward-wave second-harmonic generation in the pulsed regime

Major difference in SHG in ordinary, positive-index materials (PIM), and BW (NIM) materials in the continuous-wave (cw) regime is summarized and illustrated in Fig. 1 [3, 4, 20]. In order to achieve phase matching, wave vectors for FH and SH must be codirected, which dictates codirected energy fluxes in PIM (Fig. 1a) and contra-directed in NIM (Fig. 1b). In a PIM, photon flux in FH depletes, whereas photon flux in SH grows across the medium so that the latter one may exceed that in FH by the exit of the NLO slab. In lossless PIM, *sum* of the photons in SH and of the photon pairs in FH is conserved in any point of the NLO media. On the contrary, FH and SH propagate in the opposite directions in a NIM. Consequently, the *difference* of the above-indicated numbers is conserved so that the number of photons $\hbar\omega_2$ at $z = L$ is always equal to zero and is less than the number of photon pairs in FH at $z = 0$ (Fig. 1c, d). The rate of the changes across the slab depends on the field strength in the input FH beam (cf. Fig. 1c, d). Figure 1e depicts dependence of the photon fluxes in the FH at the exit of the NLO slab and for SH at the exit, $z = L$, for the PIM slab and photon flux of SH from the *opposite*, $z = 0$, edge of the NIM slab. Obviously, the outlined properties of SHG in the case of ordinary FH and BW SH are similar. Figure 1a–e exhibits fundamental differences in the properties of the SHG which involves backward light as compared to the SHG in ordinary crystals.

Unparalleled properties of BWSHG in the pulsed regime stem from the fact that it occurs only inside the traveling pulse of fundamental radiation. Generation begins on the leading edge of the pulse, grows toward its trailing edge, and then exits the pulse with no further changes. Since the fundamental pulse propagates across the slab, the duration

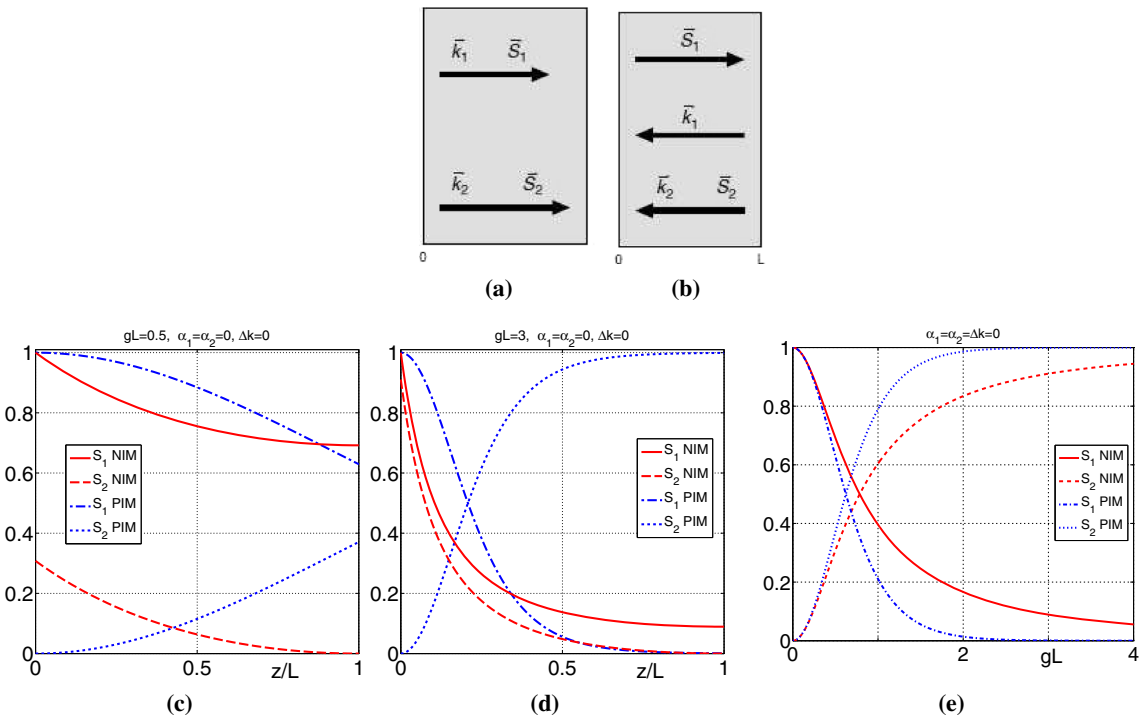

Fig. 1 Fundamental difference in the properties of continuous-wave phase-matched SHG in a loss-free ordinary and BW materials. **a**, **b** Difference in the NLO coupling and photon fluxes $S_{1,2}$ geometries. **c**, **d** Photon fluxes reduced by the input magnitudes across the slab. Here, the *descending dash-dotted blue line* depicts FH flux S_1 and the *ascending dotted blue line* depicts S_2 for SH, and both correspond to ordinary waves in a positive-index (PIM) material. The *descending solid red line* depicts S_1 flux for *backward-wave* FH, whereas the *descending dashed red line* depicts ordinary-wave S_2 flux for SH, both in a frequency double-domain positive/negative-index (NIM) slab. **c** $gL = 0.5$, **d** $gL = 3$. **e** Output transmitted fundamental (the *descending blue dash-dotted line*) and SH (the *ascending blue dotted line*) fluxes at $z = L$, both are ordinary waves in a PIM. The *descending solid red line* displays transmitted BW flux S_1 at $z = L$, and the *ascending dashed red line* depicts output ordinary SH flux at $z = 0$, both correspond to a NIM

of the SH pulse is expected to be longer than that of the fundamental one. Depletion rate of the FH radiation across its pulse length and the conversion efficiency must depend on its initial maximum intensity, and phase and group velocity matching. Ultimately, the overall properties of BWSHG such as the output pulse length and the photon conversion efficiency can be foreseen dependent on the ratio of the fundamental pulse and slab lengths. Investigation of the indicated dependence is the major goal of this work.

The input pulse shape is chosen close to a rectangular form

$$F(\tau) = 0.5\left(\tanh\frac{\tau_0 + 1 - \tau}{\delta\tau} - \tanh\frac{\tau_0 - \tau}{\delta\tau}\right), \qquad (11)$$

where $\delta\tau$ is the duration of the pulse front and tail, and τ_0 is the shift of the front relative to $t = 0$. Parameters $\delta\tau = 0.01$ and $\tau_0 = 0.1$ were selected for numerical simulations based on the system of partial differential Eqs. (7) and (8). The results are illustrated in Figs. 2 and 3. A rectangular shape of the fundamental pulse, $T_1 = |a_1(z)|^2/|a_{10}|^2$, is shown at $z = 0$ when its leading front enters the medium and the results of numerical simulations for the output fundamental pulse when its tail reaches the slab boundary at $z = L$. Shape and conversion efficiency of the output SH pulse, $\eta_2 = |a_2(z)|^2/|a_{10}|^2$, traveling against the z-axis are shown when its tail passes the slab's edge at $z = 0$. Here, phase and group velocities of the fundamental and SH pulses assumed equal. Figure 2a corresponds to the fundamental pulse of ten times and Fig. 2b of two times longer than the slab thickness. Losses are neglected. It is seen that pulse shapes of SH are significantly different in (a) and (b) cases. It is because the transient periods when only part of the fundamental pulse is inside the slab are longer relative to its duration in the second case. Since the metaslab is lossless, the outlined properties satisfy the conservation law: the number of annihilated pair of photons of in the FH $(S_{10} - S_{1L})/2$ per pulse is equal to the number of output SH photons S_{20}. Here, $S_{1,2}(z)$ are numbers of photons integrated over the corresponding pulse duration and normalized by the corresponding integrated input numbers. Note that maximum possible photon conversion efficiency for SH is 0.5. Figure 2c, d shows effect of losses which roughly correspond to one of the models of the metaslab made of free-standing carbon nanotubes [9–11]. Figure 3a, b illustrates the effect of further pulse shortening. Here, Fig. 3a displays input pulse five times and Fig. 3b—ten times, shorter than the metaslab thickness. From comparing Figs. 2 and 3, one concludes that difference in the pulse lengths grows so that SH pulse becomes much longer compared to the FH pulse. Counterintuitively, quantum conversion efficiency per pulse decreases with decrease in

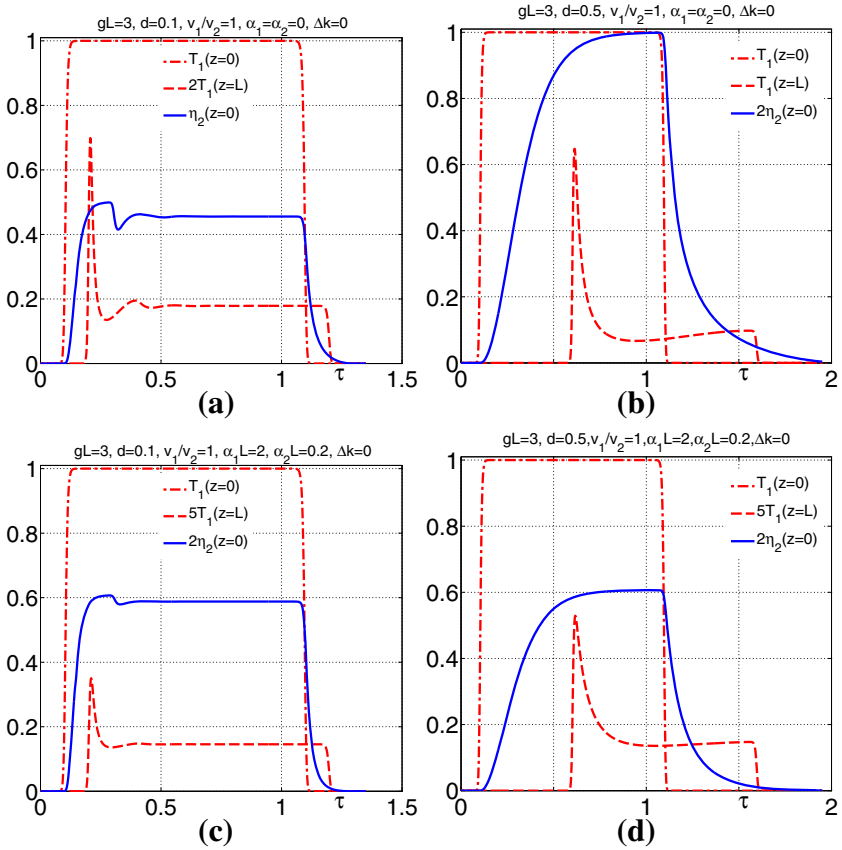

Fig. 2 Backward-wave second-harmonic generation in the pulse regime. The *red dash-dotted plot* depicts input (at $z = 0$) pulse of FH, and the *red dashed plot* depicts transmitted pulse at $z = L$. The *blue solid plot* depicts output contra-propagating pulse at doubled frequency at $z = 0$. $\tau = t/\Delta\tau$, $gL = 3$, $d = L/l$. **a**, **b** Losses are neglected. **c**, **d** $\alpha_1 L = 2$, $\alpha_2 L = 0.2$. **a**, **c** $d = 0.1$. **b**, **d** $d = 0.5$. $S_1(0) = 0.9900$. **a** $S_1(L) = 0.0934$, $S_2(0) = 0.4485$. **b** $S_1(L) = 0.1117$, $S_2(0) = 0.4391$. **c** $S_1(L) = 0.03$, $S_2(0) = 0.2865$. **d** $S_1(L) = 0.0343$, $S_2(0) = 0.2695$

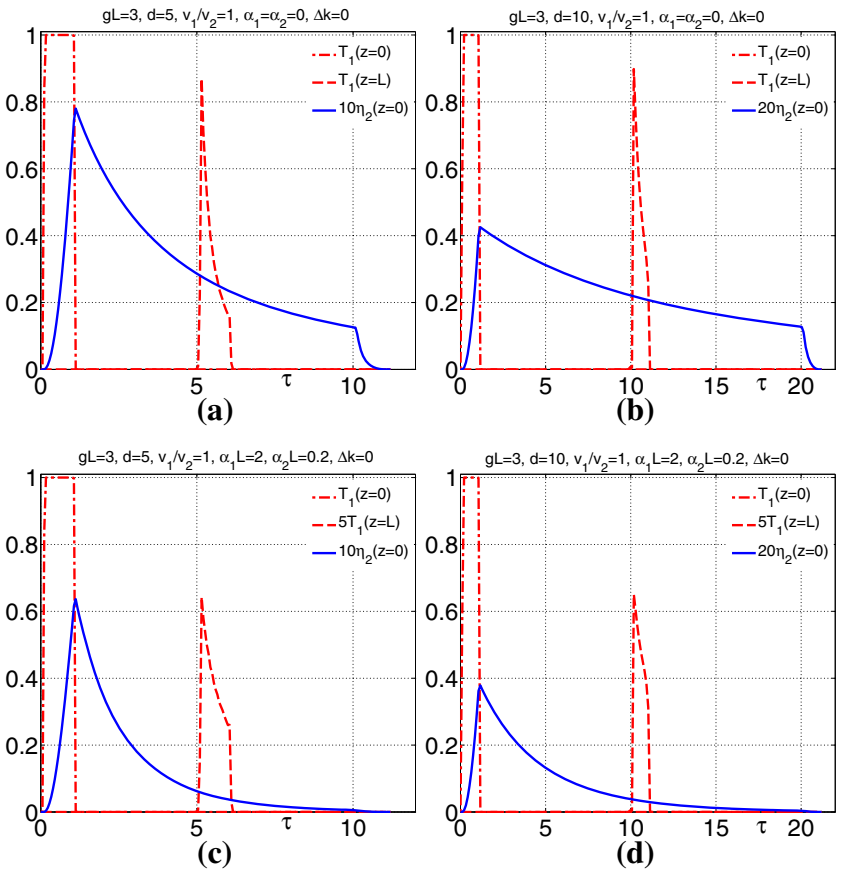

Fig. 3 Input, transmitted and reflected pulses. **a**, **c** $d = 5$, **b**, **d** $d = 10$. $S_1(0) = 0.9900$. **a** $S_1(L) = 0.3607$, $S_2(0) = 0.3111$. **b** $S_1(L) = 0.5116$, $S_2(0) = 0.2403$. **c** $S_1(L) = 0.0734$, $S_2(0) = 0.1273$. **d** $S_1(L) = 0.0923$, $S_2(0) = 0.0787$. Notations and other parameters are the same as in Fig. 2

the input pulse duration even though its maximum field strength remains unchanged and losses change SH pulse shape.

4 Conclusions

The properties of frequency-doubling nonlinear-optical metamirror operating in pulsed regime are investigated. The metamirror is proposed to be made of the metamaterial which supports backward light wave at one of the frequencies and ordinary wave at another frequency. The phase velocities are supposed adjusted equal and codirected, whereas the energy fluxes of the pump and generated second-harmonic light are contra-directed. References are given to the works that prove such a possibility. Hence, the proposed concept enables tailored, frequency shifting *reflectivity* which is fundamentally different from the standard, forward-wave second-harmonic generation. Estimations show that intensities of the pump wave, which are required to achieve significant conversion efficiency with account for losses and miniature dimensions of the mirror, may appear above the optical breakdown threshold, whereas it is not the case for pulsed lasers. Physical principles underlying differences in the properties of second-harmonic generation in the proposed and standard settings as well as between continuous-wave and pulsed regimes are discussed. A set of partial differential equations which describe such a reflector with the account for losses are written and solved numerically. It is shown that unlike second-harmonic generation in standard settings, contra-propagating generated second-harmonic pulse may become much longer than the incident fundamental one and the difference grows with decrease in the input pulse length as compared to thickness of the metaslab. The revealed properties are important for applications and may manifest themselves beyond the optical wavelength range.

Acknowledgments This material is based upon work supported in part by the US Army Research Laboratory and the US Army Research Office under Grant Number W911NF-14-1-0619, by the National Science Foundation under Grant Number ECCS-1346547 and by the Russian Foundation for Basic Research under Grant RFBR 15-02-03959A. We thank I. S. Nefedov, A. E. Boltasseva, and V. M. Shalaev for inspiring inputs.

References

1. W. Cai, V. Shalaev, *Optical Metamaterials, Fundamentals and Applications* (Springer, New York, 2010)

2. I.V. Shadrivov, A.A. Zharov, Yu.S. Kivshar, Second-harmonic generation in nonlinear left-handed metamaterials. JOSA B **23**, 529–534 (2006)
3. A.K. Popov, V.V. Slabko, V.M. Shalaev, Second harmonic generation in left-handed metamaterials. Laser Phys. Lett. **3**, 293–296 (2006)
4. A.K. Popov, V.M. Shalaev, Negative-index metamaterials: second harmonic generation, Manley–Rowe relations and parametric amplification. Appl. Phys. B. **84**, 131–137 (2006)
5. A.K. Popov, V.M. Shalaev, Compensating losses in negative-index metamaterials by optical parametric amplification. Opt. Lett. **31**, 2169–2171 (2006)
6. A.K. Popov, S.A. Myslivets, Nonlinear-optical metamirror. Appl. Phys. A **103**, 725–729 (2011)
7. A. Rose, Da Huang, D.R. Smith, Controlling the second harmonic in a phase-matched negative-index metamaterial. Phys. Rev. Lett. **107**, 063902–063904 (2011)
8. H. Suchowski, K. OBrien, Z.J. Wong, A. Salandrino, X. Yin, X. Zhang, Phase mismatch-free nonlinear propagation in optical zero-index materials. Science **342**, 1223–1226 (2013)
9. A.K. Popov, M.I. Shalaev, S.A. Myslivets, V.V. Slabko, I.S. Nefedov, Enhancing coherent nonlinear-optical processes in nonmagnetic backward-wave materials. Appl. Phys. A **109**, 835–840 (2012). doi:10.1007/s00339-012-7390-8
10. A.K. Popov, M.I. Shalaev, V.V. Slabko, S.A. Myslivets, I.S. Nefedov, Nonlinear backward-wave photonic metamaterials. Adv. Sci. Technol. **77**, 246–252 (2013). doi:10.4028/www.scientific.net/AST.77.246
11. A.K. Popov, V.V. Slabko, M.I. Shalaev, I.S. Nefedov, S.A. Myslivets, Nonlinear optics with backward waves: extraordinary features, materials and applications. Solid State Phenom. **213**, 222–225 (2014). doi:10.4028/www.scientific.net/SSP.213.222
12. V.M. Agranovich, Y.R. Shen, R.H. Baughman, A.A. Zakhidov, Linear and nonlinear wave propagation in negative refraction metamaterials. Phys. Rev. B **69**, 165112 (2004)
13. V.M. Agranovich, Yu.N. Gartstein, Spatial dispersion and negative refraction of light. Physics-Uspekhi (UFN) **176**, 10511068 (2006). (also in Physics of Negative Refraction, C.M. Krowne, Y. Zhang (Eds.), Springer, 2007)
14. I.V. Lindell, S.A. Tretyakov, K.I. Nikoskinen, S. Ilvonen, BW media—media with negative parameters, capable of supporting backward waves. Microw. Opt. Technol. Lett. **31**, 129–133 (2001). doi:10.1002/mop.1378
15. I. Nefedov, S. Tretyakov, Ultrabroadband electromagnetically indefinite medium formed by aligned carbon nanotubes. Phys. Rev. B **84**, 113410–113414 (2011)
16. E.E. Narimanov, Photonic hypercrystal. Phys. Rev. X **4**, 041014 (2014)
17. C. Duncan, L. Perret, S. Palomba, M. Lapine, B.T. Kuhlmey, C. Martijn de Sterke, New avenues for phase matching in nonlinear hyperbolic metamaterials. Sci. Rep. **5**, 8983 (2015). doi:10.1038/srep08983
18. S. Mokhov, R. El-Ganainy, D.N. Christodoulides, Power circulation via negative energy-flux wormholes in optical nanowaveguides. Opt. Express **14**, 3255–3262 (2006)
19. A. Salandrino, D.N. Christodoulides, Negative index Clarricoats–Waldron waveguides for terahertz and far infrared applications. Opt. Express **18**, 3626–3631 (2010)
20. A.K. Popov, S.A. Myslivets, Second harmonic generation and pulse shaping in positively and negatively spatially dispersive nanowaveguides: comparative analysis. arXiv:1507.07167